VISCOUS BOUNDARY LAYER MEASUREMENTS IN RAYLEIGH-BENARD CONVECTION

Ke-Qing Xia
Department of Physics, The Chinese University of Hong Kong
Shatin, New Territories, Hong Kong

Abstract

Aimed at understanding the large scale circulation found in the so-called hard-turbulence regime of Rayleigh-Bénard convection and its interaction with boundary layers, we have performed precision velocity profile measurements in high Rayleigh number (Ra) turbulent convection. Our measured velocity profile as a function of Ra reveal that the shear rate (γ), the viscous boundary thickness (δ_v), and the maximum velocity (v_m) all follow a power law of Ra with respective exponents of 0.66, -0.16 and 0.5.

The discovery of the hard turbulence regime[1] has stimulated much interests in Rayleigh-Bénard convection recently[2]. The hard turbulence state at the Rayleigh number Ra > 4×10^7 is characterized by scaling laws in the heat flux and temperature statistics and also by a coherent large-scale circulation that spans the height of the convection cell. It has been widely recognized that the thermal and viscous boundary layers near the upper and lower surfaces of the cell play an important role in determining the heat flux and temperature statistics[3-5]. Direct measurements of the boundary layer properties, therefore, become essential to the understanding of convective turbulence. In contrast to many thermal boundary layer measurements[3,4,6], however, experimental information about viscous boundary layers in turbulent convection is limited. The lack of the velocity information is partially due to the fact that the conventional methods for measuring velocity such as hot-wire anemometry and laser Doppler velocimetry (LDV), are not suitable for thermal turbulence. Recently, Tilgner et. al. have used an imaging technique to measure the velocity profile near the top plate of a cubic cell filled with water[6]. Because of the cumbersome procedure of the method, the velocity measurement was conducted only at a single value of Ra (~10^9).

We report here results of direct measurements of the velocity boundary layer properties for turbulent convection in water with Ra ranging from 10^7 to 10^{10}. A novel light scattering technique of dual-beam incoherent cross-correlation spectroscopy[7] is used to measure the velocity profile v(z) as a function of the distance z from the lower surface of the cell. In the experiment two parallel laser beams with a known separation l are shone through the convecting fluid. The two beams are the blue and green lights from an argon-ion laser operated under the multiline mode. The fluid is seeded with neutrally buoyant polymer latex spheres of 0.95 μm in diameter. These particles scatter light and follow the motion of the fluid. The velocity of the seed particles is determined by measuring the time required for the particles to cross the two parallel beams in succession. Experimentally, this transit time, or delay time, is obtained from the cross-correlation function[7]

$$g_c(t) = \frac{<I_b(t')I_g(t'+t)>}{<I_b><I_g>} = 1+\beta G_c(t) \tag{1}$$

between the scattered intensities $I_b(t)$ and $I_g(t)$, from the blue and green beams respectively. In Eq. (1), β is an instrumental constant. Because there is no phase coherence between $I_b(t)$ and $I_g(t)$, $g_c(t)$ is sensitive only to the scattering amplitude fluctuations produced by the seed particles moving in and out of the laser beams. For a turbulent flow, $G_c(t)$ in Eq. (1) should be averaged over the probability density function (PDF) P(v) of the local velocity v. If P(v) is assumed to have a Gaussian form, $G_c(t)$ then becomes[8]

$$G_c(t) = \frac{1}{N\sqrt{1+2(\sigma t/r_0)^2}} e^{-(v_0 t-l)^2/[r_0^2+2(\sigma t)^2]} \tag{5}$$

In the above, v_0 is the mean velocity, σ the standard deviation, r_0 the beam radius, and N the average number of particles in the scattering volume.

The convection cells used were vertical cylinders of 19 cm in diameter with gold-plated upper and lower copper plates. The sidewall of the cells were cylindrical rings made of transparent plexiglas. Two cylindrical rings with heights 9.4 cm and 19.6 cm were used, respectively, to extend the accessible range of Ra. The corresponding aspect ratios (A=diameter/height) for the two cells are approximately 2 and 1. The temperature of the upper plate was regulated by passing cold water through a cooling chamber fitted on the top of the plate. The lower plate was heated uniformly at a constant rate with an imbedded film heater. The temperature difference ΔT between the two plates was measured by two thermistors imbedded in the plates. The control parameter in the experiment is the Rayleigh number $Ra=\alpha g h^3 \Delta T/\nu\kappa$, with α being the thermal expansion coefficient, g the gravitational acceleration, h the height of the cell, ν and κ the kinematic viscosity and the thermal diffusivity of the fluid, respectively.

The details of the technique has been described elsewhere[7], here we show only the schematic experimental setup in Fig. 1. A lens was used to focus the two laser beams emerging from a prism into the convection cell. The two beams become parallel after passing through the lens, and they were horizontally shone through the center of the cell. A second lens was placed at 90^0 with respect to the incident direction of the beams, and projected the images of the scattered beams in the cell onto an adjustable slit (width = 0.3 mm in experiment) with a 1:1 magnification. The slit was so positioned such as only the center portion of the scattered beams were seen by two photomultipliers (PM) placed behind it. Aided by a beamsplitter and two interference filters, one of the PM detects only $I_b(t)$ and the other $I_g(t)$. The output pulse trains from the two PM's were fed to a digital correlator, which gives $g_o(t)$. The convection cell can be moved vertically to change the distance z between the beams and the lower surface of the cell. The orientation of the plane defined by the two beams was adjusted to be either parallel or perpendicular to the lower surface, so that the horizontal and vertical components of the local velocity could be measured, respectively. The beam separation *l* was fixed at 0.22 mm in the experiment.

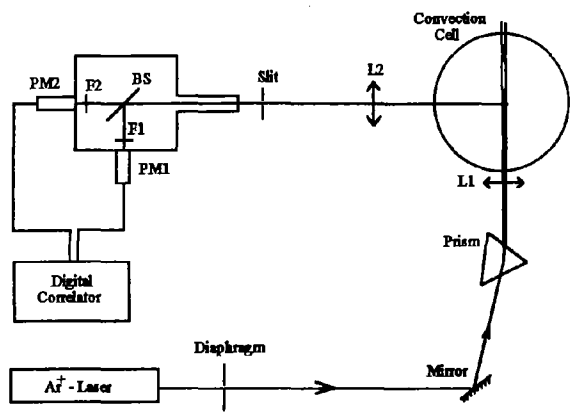

Fig. 1 Schematic diagram of the experimental setup. F1 and F2 are interference filters (488 nm and 514.5 nm), BS is a beamsplitter, PM1 and PM2 are photomultiplers, and L1, L2 are lenses.

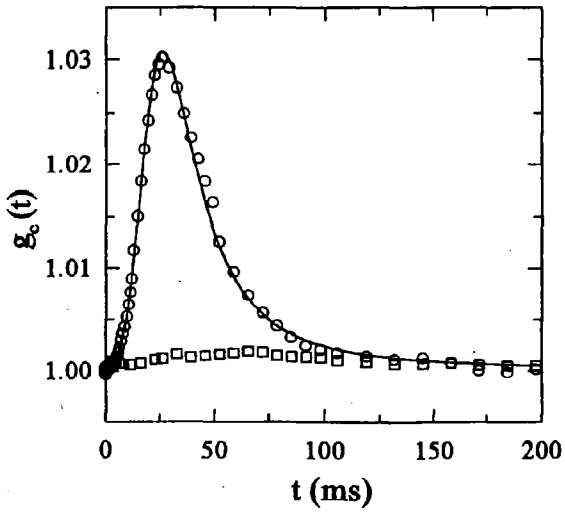

Fig. 2 Measured "green cross blue" (circles) and "blue cross green" (squares) cross-correlation functions $g_o(t)$ at $Ra=1.82\times10^9$ and z = 3.0 mm. The solid curve is a fit of Eq. (2) to the circles.

Figure 2 shows two cross-correlation functions measured simultaneously at $Ra=1.8\times10^9$, when the correlator was operated under the ``dual-cross" mode. The circles represent a ``green-cross-blue" correlation function (GCB), in which the measured $I_b(t)$ was delayed relative to $I_g(t)$. The squares represent a ``blue-cross-green" correlation function (BCG). In this measurement the two beams lay in a plane parallel to the plates of the cell so that only the horizontal velocity v_h was measured. The cell was also rotated about its central vertical axis so that a

maximum value of v_h was achieved. It is clearly seen from Fig. 2 that GCB is a Gaussian-like function, whereas BCG is essentially a constant baseline. This indicates that v_h is uni-directional near the boundary, and its direction is such that the seed particles first passed through the green beam and then the blue one. The solid line in Fig. 1 shows the fit of Eq. (2) to the measured GCB with v_0=0.89 cm/s and σ=0.3 cm/s. We have found that the measured $G_o(t)$ at different values of z and Ra can all be fitted to Eq. (2). Figure 2 thus suggests that the P(v) near the boundary has a Gaussian form. Gaussian-type PDF's have also been found in the center region of the convection cell[9]. The vertical velocity v_v is also measured near the boundary at various Ra. Within the sensitivity of the technique, we find v_v to be negligible.

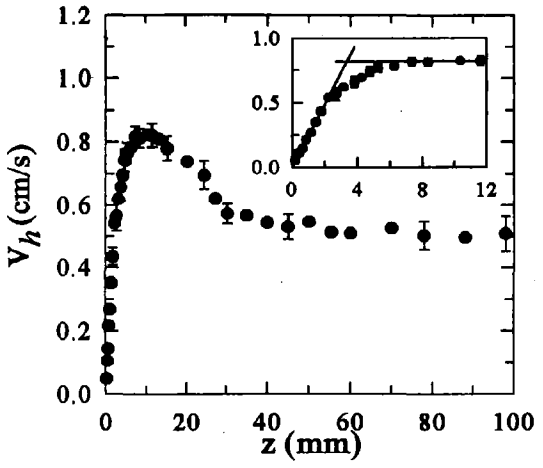

Fig. 3 Measured velocity profile at Ra=9.24×10^8 along the central axis of convection cell. The inset shows an enlarged portion of the profile near boundary.

Figure 3 shows the measured $v_h(z)$ at Ra=9.24x10^8. The values of $v_h(z)$ were obtained by fitting Eq. (2) to the measured correlation functions and were determined mainly by the peak positions of $G_o(t)$. It is seen that $v_h(z)$ increases with z for small values of z. After it reaches the maximum value v_m, $v_h(z)$ decays when z is further increased toward the cell center. The measured $v_h(z)$ shows similar features as those from a previous measurement at Ra~10^9 using an imaging technique[6]. As shown in the inset of Fig. 3, the measured $v_h(z)$ near the boundary can be well described by a linear function of z with a zero intercept (non-slip boundary condition). The slope of the linear function is the shear rate γ. The thickness δ_v of the viscous boundary layer is defined as the distance at which the extrapolation of the linear part of $v_h(z)$ equals v_m, or simply $\delta_v = v_m/\gamma$. It is found that all velocity profiles measured for different Rayleigh numbers $v_h(z)$ can be brought into coincidence, once the velocity $v_h(z)$ is scaled by v_m(Ra) and the distance z by δ_v(Ra).

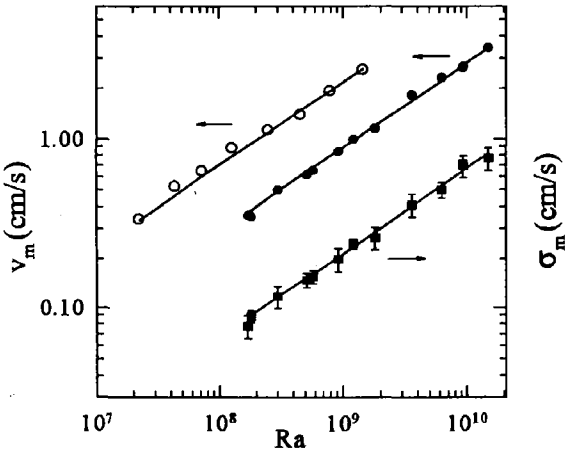

Fig. 4 Maximum horizontal velocity v_m (circles) and its standard deviation σ_m (squares) as functions of Ra measured from two cells (solid symbols: A=1, open symbols: A=2).

We now examine the Ra-dependence of the characteristic quantities of the boundary layer: v_m, γ and δ_v. In Fig. 4 we show the measured v_m and its standard deviation σ_m plotted against Ra. For clarity, only σ_m for A=1 cell are shown. As can be seen, all data can be described by parallel straight lines in the log-log plot. The corresponding power law fits are v_m=3.1x10^{-5}Ra$^{0.5}$ cm/s and σ_m = 7x10^{-6} Ra$^{0.5}$ cm/s for A=1 cell (solid symbols), and v_m = 7.5x10^{-5}Ra$^{0.5}$ cm/s for A=2 cell (open symbols). It should be pointed out that the measured v_m is the speed of the large-scale circulation or the wind that sweeps over the surfaces of the cell and shears the thermal boundary layers. If the Peclet number Pe (=$v_m h/\kappa$) is chosen as a dimensionless velocity, we find from Fig. 4 that Pe = 0.42 Ra$^{0.5}$ and 0.54 Ra$^{0.5}$ for the A=1 and 2 cells respectively. Figure 5 shows the shear rate γ as a function of Ra measured from the two cells (solid circles: A=1, open circles: A=2). The data are well described by γ = 2.6x10^{-6} Ra$^{0.66}$ s^{-1} (A=1) and γ = 9.86x10^{-6}Ra$^{0.66}$ s^{-1} (A=2). With the measured γ(Ra) and Nu(Ra), we find Nu~$\gamma^{0.44}$. This result does not support the scaling relation Nu~$\gamma^{1/3}$ predicted by a recent model[5] partly aimed at deriving the power law Nu~Ra$^{2/7}$. In Fig. 6 we show the measured viscous boundary

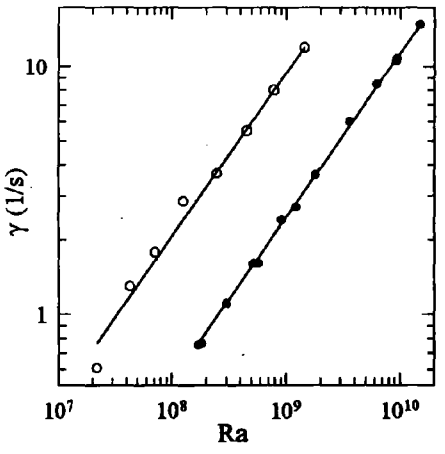

Fig. 5 Measured shear rate γ versus Ra. Solid dots: data from A=1 cell, open circles: data from A=2 cell. The upper straight line is a power law fit of $\gamma = 9.86\times10^{-6}\,Ra^{0.66}$, the lower straight line is $\gamma = 2.6\times10^{-6}\,Ra^{0.66}$.

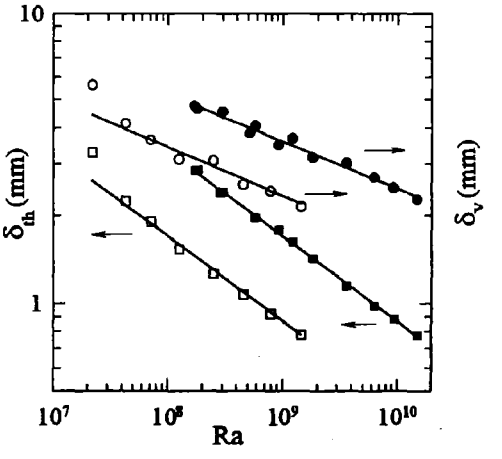

Fig. 6 The viscous boundary layer thickness δ_v (circles) and the thermal layer thickness δ_{th} (squares) measured, respectively, from A=1 cell (solid symbols) and A=2 cell (open symbols).

layer thickness δ_v versus Ra for the two cells (solid circles: A=1, open circles: A=2). The power law fits are $\delta_v = 10.1\ Ra^{-0.16}$ cm (A=1) and $\delta_v = 6.7\ Ra^{-0.16}$ cm (A=2). It is seen from Fig. 6 that δ_v decays as $Ra^{-0.16}$, and we do not observe any abrupt changes, as suggested by a recent temperature measurement[6]. For comparison, we also plot in Fig. 6 the thermal boundary layer thickness δ_{th} (squares), which is obtained from the measured Nu using the well-tested relation[6] $\delta_{th} = h/(2Nu)$. This thickness is well fitted by $\delta_{th} = 70.0\ Ra^{-0.291}$ mm (A=1) and $\delta_{th} = 36.2\ Ra^{-0.291}$ mm (A=2). As shown in Fig. 6 the thermal boundary layer is nested within the viscous boundary layer for both cells in our working range of Ra. Clearly, if the current trend for δ_v and δ_{th} continues, the viscous and thermal boundary layers would not crossover at higher Ra, as suggested by a recent model[5].

In summary, our direct measurements of the viscous boundary layer properties demonstrate that previous extrapolations and speculations, based on temperature measurements, for the scaling velocity[3], the viscous boundary layer thickness[6], and the shear rate[4] are not reliable. And further studies of the boundary layer dynamics, both experimental and theoretical are needed in order to develop a more fundamental understanding of thermal turbulence.

My coworker in this experiment is Mr. Yongbao Xin who did most of the measurements. I also thank my collaborator Penger Tong for helpful discussions.

References:

[1] F. Heslot, B. Castaing and A. Libchaber, Phys. Rev. A, **36**, 5870 (1987); B. Castaing *et al*, J. Fluid Mech., **204**, 1 (1989).
[2] see, for example, E. D. Siggia, Annu. Rev. Fluid Mech., **26**, 137 (1994), and references therein.
[3] T. H. Solomon and J. P. Gollub, Phys. Rev. Lett., **64**, 2382 (1990); Phys. Rev. A, **43**, 6683 (1991); B. J. Gluckman, H. Willaime and J. P. Gollub, Phys. Fluids, **5**, 647 (1993).
[4] F. Chilla, S. Ciliberto and C. Innocenti, Europhys. Lett., **22**, 681 (1993).
[5] B. I. Shraiman and E. D. Siggia, Phys. Rev. A, **42**,3650 (1990).
[6] A. Tilgner, A. Belmonte and A. Libchaber, Phys. Rev. E, **47**, R2253 (1993); Phys. Rev. Lett., **70**, 4067 (1993); Phys. Rev. E, **50**, 269 (1994).
[7] K.-Q. Xia, Y.-B. Xin and P. Tong, J. Opt. Soc. Amer. A, **12**, 1571 (1995).
[8] Y.-B. Xin, K.-Q. Xia, and P. Tong, submitted to Phys. Rev. Letts.
[9] Y. Shen, K.-Q. Xia, and P. Tong, Phys. Rev. Letts., **75**, 437 (1995).